BACHELOR

Stabilization of the inverted pendulum

Maas, Wietse J.A.

Award date:
2022

Department of Mechanical Engineering
Dynamics and Control
PO Box 513, 5600 MB Eindhoven
The Netherlands
www.tue.nl

Stabilization of the inverted pendulum

Author
W.J.A. Maas (1459090)

Supervisor
A. Pogromsky

Date
June 24, 2022

Abstract

A regular pendulum has two equilibrium positions; its bottom position and its top position. When its pivot is fixated, only the bottom equilibrium position is regarded stable. This changes when the pendulum's pivot is being vertically oscillated with appropriate amplitude and frequency. The pendulum might become stable in top equilibrium position and unstable in bottom equilibrium position. In this report, this phenomenon is investigated. First, a stability analysis is performed and a model is developed describing the pendulum's (in)stability. This model is successfully validated by conducting an experiment. Afterwards, the pendulum is simulated using an ODE solver in Matlab. The results from both the developed model and the computer simulation are then used to design and build an experimental setup in which an inverted pendulum is being stabilized. Lastly, an experiment is conducted using the created setup and the results are being compared to both the model and the simulation.

EINDHOVEN UNIVERSITY OF TECHNOLOGY

Table of contents

Title
Stabilization of the inverted pendulum

Introduction

Dynamic stability of an ordinary pendulum can be approached in an intuitive manner. The pendulum has two equilibrium positions; one at its bottom and one at its top position, where generally only one of them is stable. Under standard conditions, that is when rotating around a fixated pivot point, the bottom position is stable and the top position is unstable. However, when the pivot point is vertically oscillated with appropriate amplitude and frequency, the stability position can shift from bottom to top equilibrium position.

This phenomenon has already been studied for over a decade. In 1908, Andrew Stephenson was the first to publish an article about the stabilization of an inverted pendulum. He found that if the pendulum is being oscillated, its top vertical position might stabilize when its oscillation frequency is fast enough [1]. This article turned out to be the starting point of several more studies to the behaviour of an inverted pendulum. It then took until 1951 for a first real explanation for this phenomenon; Pyotr Kapitza was the first to develop a theory to support inverted pendulum stability [2].

This project aims to achieve three fundamental objectives. First of all, the behaviour of an inverted pendulum should be modelled and a validation experiment has to confirm the theoretical conclusions (objective 1). Second of all, a computer simulation should be developed that mimics the pendulum with a reasonable accuracy (objective 2). Lastly, based on theoretical results from the model and the simulation, an experimental setup should be designed and built which demonstrates the investigated phenomenon (objective 3).

The report will begin by setting up the pendulum's equation of motion using the Euler-Lagrange equations. This equation of motion can be linearized, after which it is simplified by applying time dependent switching to the pivot's acceleration. With these equations set up and its resulting solution, stability criteria are established and an experiment is conducted to validate the model. Afterwards, the report will elaborate on a computer simulation of the inverted pendulum and a comparison will be made to the earlier developed model. The combination of resulting data from both the model and the computer simulation will ultimately be used to develop an experimental setup stabilizing an inverted pendulum. Finally, the report concludes with a comparison between the observed results from this setup and the theoretical results from model and simulation, after which a final conclusion will be drawn.

1 Develop inverted pendulum model

In order to be able to understand the behaviour of a vertically oscillated inverted pendulum, a stability analysis is performed. After the situation has been introduced, the pendulum equation of motion is being set up using the Euler-Lagrange equation. Afterwards, by utilizing this equation of motion and assuming time-dependent switching for the vertical oscillation one can derive conditions for potential pendulum instability in lower position.

1.1 Situation description

For this theoretical stability analysis, the inverted pendulum consists of a point mass M connected to a rod of length L and negligible mass. The rod rotates around a pivot point which is vertically oscillated. This oscillation behaviour is defined by the function $s(t)$, which is a function of time. The exact shape of this function is yet undefined. The clockwise-positive angle the pendulum makes with the vertical is defined as φ, which is set zero at the top position. The situation is sketched in Figure 1.1.1 with corresponding 2D coordinate system.

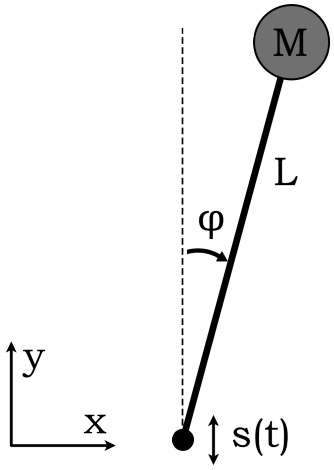

Figure 1.1.1: Situation sketch vertically oscillated inverted pendulum

1.2 Equation of motion

Continuing from Figure 1.1.1, the pendulum's equations of motion can be derived. This is done in several sub steps, which will all be elaborated in this section.

Point mass position and its time derivative

To start off the stability analysis, the x and y position of the point mass is expressed in known quantities. To do so, first an origin is defined; this is the pivot point in initial position. From here it can be derived that

$$x = \sin(\varphi)L \tag{1.1}$$
$$y = \cos(\varphi)L + s(t) \tag{1.2}$$

from which it directly follows that the time derivative of this position is defined as

$$\dot{x} = \dot{\varphi}\cos(\varphi)L \tag{1.3}$$
$$\dot{y} = -\dot{\varphi}\sin(\varphi)L + \dot{s}(t) \tag{1.4}$$

Kinetic and potential energy and the Euler-Lagrange equation

Now the pendulum's x and y positions and their time derivatives have been expressed in known quantities, the pendulum's kinetic and potential energy can be derived. This is done using the regular equations for kinetic and potential energy.

$$E_k = \frac{1}{2}M(\dot{x}^2 + \dot{y}^2) = \frac{1}{2}M(\dot{\varphi}^2L^2 - 2\dot{\varphi}\sin(\varphi)L\dot{s} + \dot{s}^2) \tag{1.5}$$
$$E_p = Mgy = Mg(\cos(\varphi)L + s) \tag{1.6}$$

In order to come to the equation of motion according the Euler-Lagrange equation, the Lagrangian ($\mathcal{L}$) is a necessary quantity. This Lagrangian is defined as the difference between kinetic and potential energy, previously computed in Equation 1.5 and Equation 1.6. This means the Lagrangian can be expressed as

$$\mathcal{L} = E_k - E_p = \frac{1}{2}M(\dot{\varphi}^2L^2 - 2\dot{\varphi}\sin(\varphi)L\dot{s} + \dot{s}^2) - Mg(\cos(\varphi)L + s) \tag{1.7}$$

after which the Euler-Lagrange equation displayed in Equation 1.8 can be applied.

$$\frac{d}{dt}\left(\frac{\partial\mathcal{L}}{\partial\dot{q}}\right) - \frac{\partial\mathcal{L}}{\partial q} = F_{nc} \tag{1.8}$$

This results in the equation of motion presented in Equation 1.9, where λ represents a damping constant. A full derivation can be found in section A.1.

$$\ddot{\varphi} + \lambda\dot{\varphi} - \frac{1}{L}(g + \ddot{s})\sin(\varphi) = 0 \tag{1.9}$$

Equilibrium positions and linearization

The nonlinear differential equation displayed in Equation 1.9 is challenging to solve analytically. The equation can be linearized around an equilibrium point to create a linear differential equation, which is more straight-forward to solve. In order to do so, first the pendulum's equilibrium points have to be obtained. This is done using the known fact that potential energy is constant at equilibrium positions. Alternatively stated, at equilibrium positions:

$$\frac{dE_p}{d\varphi} = 0 \tag{1.10}$$

Using Equation 1.6, the two equilibrium positions logically are found to be $\varphi = 0 + k \cdot 2\pi$ and $\varphi = \pi + k \cdot 2\pi$, corresponding to the top and bottom position of the pendulum respectively. The calculation can be found in section A.2.

This stability analysis will focus on the instability of the pendulum's bottom position because this matches with the experimental setup which will be used later to validate the model. Therefore, Equation 1.9 will be linearized around this bottom equilibrium position to get the linear equation of motion. The worked out linearization process is shown in section A.3. This results in the following differential equation, describing the linearized pendulum's equation of motion around the bottom position:

$$\ddot{\theta} + \lambda\dot{\theta} + \frac{1}{L}(g + \ddot{s})\theta = 0 \tag{1.11}$$

1.3 Stability Analysis

As the pendulum's linearized equation of motion is now obtained, the intended stability analysis can be conducted. This analysis is described in this section.

Second order to first order and definition of s(t)

In order to simplify stability analysis criteria, the second order differential equation seen in Equation 1.11 is converted to a first order differential equation. This results in the following differential equation:

$$\frac{d}{dt}\begin{bmatrix}\theta \\ \dot{\theta}\end{bmatrix} = \begin{bmatrix}0 & 1 \\ -\frac{1}{L}(g + \ddot{s}) & -\lambda\end{bmatrix}\begin{bmatrix}\theta \\ \dot{\theta}\end{bmatrix} \tag{1.12}$$

This equation can now be used to perform a stability analysis. To do so, first the exact behaviour of the pivot oscillation function $s(t)$ should be defined. For practical reasons, the function is set to be equal to $s(t) = A\sin(\omega t)$. Equation 1.12 then becomes:

$$\frac{d}{dt}\begin{bmatrix}\theta \\ \dot{\theta}\end{bmatrix} = \begin{bmatrix}0 & 1 \\ -\frac{1}{L}(g - \omega^2 A\sin(\omega t)) & -\lambda\end{bmatrix}\begin{bmatrix}\theta \\ \dot{\theta}\end{bmatrix} \tag{1.13}$$

To reference in the upcoming sections, this two by two matrix will be named as $B(t)$. This means Equation 1.13 has the general form

$$\dot{x} = B(t)x \quad \text{with} \quad x = \begin{bmatrix}\theta \\ \dot{\theta}\end{bmatrix} \quad \text{and} \quad B(t) = \begin{bmatrix}0 & 1 \\ -\frac{1}{L}(g - \omega^2 A\sin(\omega t)) & -\lambda\end{bmatrix}$$

Time dependent switching

For this theoretical stability analysis, however, the acceleration of the pivot is going to be approximated as a piece-wise constant function of time. Using this method results in a time-dependent switching system, for which clear stability criteria can be set. To do so, a period $T = \frac{\omega}{2\pi}$ of one full sine wave is defined. During this period, $\sin(\omega t)$ is approximated as:

$$\sin(\omega t) = \begin{cases} 1, & i = 1 \\ -1, & i = 2 \end{cases} \quad \text{with} \quad i = \begin{cases} 1, & 0 \leq t < \frac{T}{2} \\ 2, & \frac{T}{2} \leq t < T \end{cases} \tag{1.14}$$

This means matrix $B(t)$ can now be split into two separate cases which both incorporate Equation 1.14:

$$B_i(t) = \begin{cases} \begin{bmatrix} 0 & 1 \\ -\frac{1}{L}(g-\omega^2 A) & -\lambda \end{bmatrix}, & i = 1 \\ \begin{bmatrix} 0 & 1 \\ -\frac{1}{L}(g+\omega^2 A) & -\lambda \end{bmatrix}, & i = 2 \end{cases} \tag{1.15}$$

Differential equation solution and stability criterion

Now, to apply a stability criterion the general solution of this differential equation is worked out and analyzed. Assume an initial condition for the system: $x(0) = x_0$. The system starts in the first time period $0 \leq t < \frac{T}{2}$ (or $i = 1$), which means matrix $B_1(t)$ can be applied. The system's solution in this mode is given by

$$x(t) = e^{B_1 t} x_0 \tag{1.16}$$

after which the second mode ($i = 2$) is reached with new solution

$$x(t) = e^{B_2 t} x\left(\frac{T}{2}\right) = e^{B_2 t} e^{B_1 \frac{T}{2}} x_0 \tag{1.17}$$

which can be rewritten to a general solution applicable for any integer k

$$x(kT) = (e^{B_2 \frac{T}{2}} e^{B_1 \frac{T}{2}})^k x_0 \tag{1.18}$$

For $t = kT$, this solution shown in Equation 1.18 satisfies the conditions of a linear time-invariant equation of discrete time:

$$\alpha(k+1) = \beta\alpha(k) \quad \text{with} \quad \alpha(k) = x(kT) \quad \text{and} \quad \beta = (e^{B_2 \frac{T}{2}} e^{B_1 \frac{T}{2}}) \tag{1.19}$$

Now, using Equation 1.19 and the appropriate stability criterion one can tell if a vertically oscillated pendulum with length L, oscillation frequency ω and amplitude A is behaving stable or unstable. A linear time-invariant equation of discrete time is known to be asymptotically stable if and only if matrix β is Schur. This means it has eigenvalues in the open unit disc on the complex plane.

It can thus be concluded that this time dependent switched system, which forms an approximation of the real situation, is stable if and only if all absolute eigenvalues of matrix β are smaller than 1.

Analysis results

The theory described above is implemented in Matlab to visualize pendulum stability for varying conditions. The full code used for this can be observed in section C.1. For this analysis, several assumptions are made. The pendulum length L is set to 0.25 m, 0.50 m and 0.75 m for three different simulations. The damping coefficient λ is set to 0.1. These values have been chosen arbitrary. As mentioned before, this analysis solely focuses on the instability of an oscillated pendulum in bottom position (i.e. $\varphi_0 \approx \pi$). The result for this analysis can be seen in Figure 1.3.1, where the dark area represents an unstable behaviour of the pendulum. On the x-axis, the normalized angular frequency is plotted. This implies a

division of the excited angular frequency by the pendulum's eigenfrequency ($w_0 = \sqrt{\frac{g}{l}}$). On the y-axis the excitation amplitude is graphed.

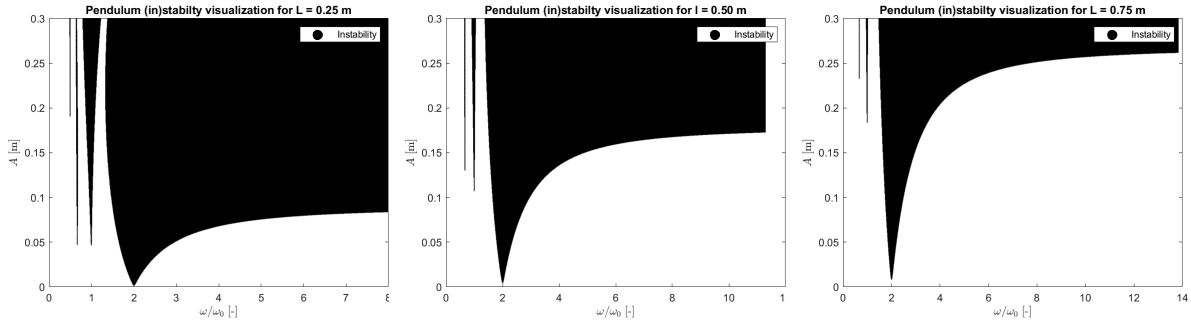

(a) L = 0.25 m (b) L = 0.50 m (c) L = 0.75 m

Figure 1.3.1: Pendulum (in)stability for varying oscillation amplitude and frequency

As can be observed in Figure 1.3.1, the described pendulum can both be stable and unstable for various combinations of length, oscillation frequency and amplitude. In general, the shorter the pendulum length the lower the required excitation amplitude in order to become unstable at relatively higher frequencies. Nevertheless, all three different pendulum lengths show similar behaviour in terms of parametric resonance. The largest peak in resonance is invariably located at $\frac{\omega}{\omega_0} \approx 2$, with several smaller resonance peaks to its left at $\frac{\omega}{\omega_0} \approx 1$ and $\frac{\omega}{\omega_0} \approx 0.67$. The right side of this largest peak does not show any resonance. This observation is in line with existing articles about this subject [3]. The results of this theoretical approach on the (in)stability of a vertically oscillated pendulum will be validated by performing an experiment, which is elaborated in chapter 2.

2 Validation experiment

In chapter 1, a model has been developed to analyze the stability of an oscillated pendulum. Although the results at first side may look realistic and are in line with existing articles about the subject, they can only be verified by performing an experiment representing the actual situation. This is done using an existing setup in the Motion laboratory at Eindhoven University of Technology. By comparing experimental results to the theoretical results obtained in chapter 1, one can tell if the stability analysis was conducted correctly.

2.1 The setup

The setup consists of a mass M connected to a rope. This rope is guided to a driving wheel via a crane-like construction. The wheel drives the mass up and down via the rope. A simplified situation sketch of the setup can be seen in Figure 2.1.1 and a picture of the actual setup can be found in Figure B.0.1.

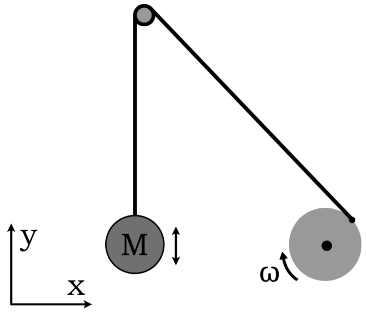

Figure 2.1.1: Simplified situation sketch experimental setup

The setup has a fixed oscillation amplitude of 0.05 m, which is equal to the radius of the driving wheel. The shortening effect of the rope as a result of the angle it makes with the line of actuation is neglected. The setup allows for oscillation frequencies from 0 rad/s to approximately 12 rad/s, which can be regulated by changing the supplied voltage to the driving wheel. Note that the pendulum's length is not a constant; it varies over time because the rope functions both as mass oscillator and as part of the pendulum. The pendulum's length can be regulated by tying knots in the rope. In this way, the length in zero-amplitude position can be varied from 0 m to approximately 0.73 m.

2.2 Pre-experimental actions

Before conducting the intended experiments with the above described setup, first several other actions are taken. This is done to get a better understanding of the setup and to interpret the results obtained later correctly. These actions include a conversion from voltage to angular frequency and determining the damping coefficient of the pendulum.

Voltage to frequency

As explained in section 2.1, the excitation frequency in the experiment can be regulated by adjusting the supplied voltage to the driving wheel. The setup includes a display which shows the voltage; this is the only output provided. This means in order to know at what frequency the pendulum is excited, the displayed voltage should be converted to an angular frequency. This is done by fixating the supplied voltage and filming the driving wheel in 60 frames per second. This action is then iterated for several

different voltages and the results are frame by frame analysed in video editing software [4]. By determining the duration of and averaging over tens of rotations of the driving wheel, the angular frequency can be accurately calculated. This results in the relation which can be observed in Figure 2.2.1a.

In the figure, the measured data points are plotted together with a linear curve fitted to the data points. It can be concluded that the resulting angular frequency behaves approximately linear with the supplied voltage. The following function, describing the red line, can now be used to convert a voltage to an angular frequency: $\omega = 1.035 \cdot V - 0.5059$.

Damping coefficient

Another yet unknown parameter in the experimental setup is the damping coefficient of the pendulum. In this setup, it is expected that largest contributor to damping will be drag. In order to find out its value, the pendulum is given an initial amplitude, after which it is released. During this operation, its pivot is not oscillated. This process is again filmed at 60 frames per second to monitor its behaviour. After the pendulum has significantly decreased amplitude, the results are analyzed and compared to an analytical solution to tune the damping coefficient. This can be seen in Figure 2.2.1b, where a damping coefficient $\lambda = 0.0079$ has been applied to the analytical solution. As can be seen, the measured data and the numerical solution approach each other closely. This means the damping coefficient for this experimental setup can now be regarded as approximately known and it can be used in the upcoming validation experiments.

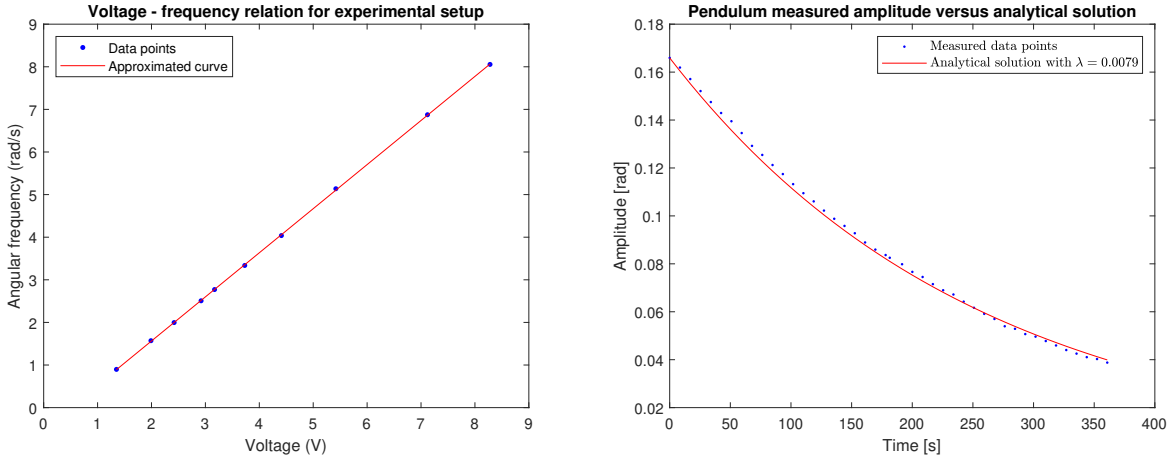

(a) Voltage-angular frequency relation

(b) Measured vs analytical amplitude for $\lambda = 0.0079$

Figure 2.2.1: Pre-experimental actions results

2.3 Experimental results and discussion

After the above described preparations have been made, the validation experiment can be carried out. The goal of the experiment is to check within which frequency domain the pendulum behaves unstable. This includes a lower limit, at which the pendulum becomes unstable when raising the frequency. Besides, if present and reachable, an upper limit is determined at which the pendulum stabilizes again when raising the frequency even further. Instability is judged by means of visual interpretation; when the mass starts shaking the pendulum is classified as unstable.

Experimental results

The experiment is conducted for six different pendulum lengths. This is done to validate if the effect of length change in the stability analysis model developed in chapter 1 coincides with the observed effect in reality. An example can be observed in Figure 2.3.1a, where the obtained pre-experimental parameters described in section 2.2 have been implemented in the stability analysis model. The pendulum length has been set to 0.5 m because this is well within the to be experimented range of lengths. The fixed amplitude of 0.05 m has been highlighted by a red horizontal line. The dark area represents the unstable pendulum area. As can be seen, for this combination of amplitude and pendulum length, there exists both an upper and a lower frequency limit. Roughly speaking, this range is from 8 to 10 rad/s in this case. This model is ran for the six different pendulum lengths at which the experiment is also conducted, after which the results form the red curves in Figure 2.3.1b.

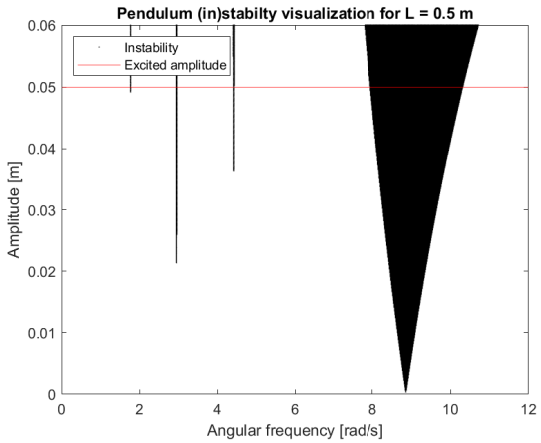

(a) Frequency instability range example

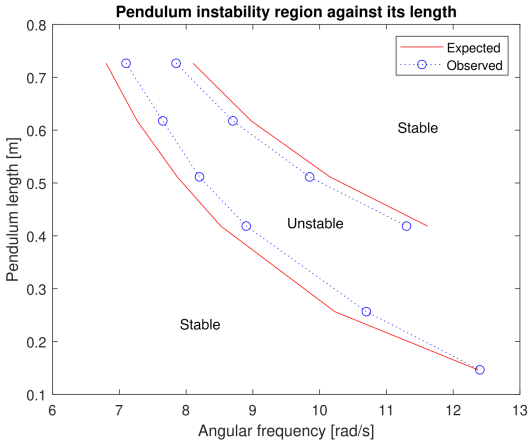

(b) Expected vs observed results for instability region

Figure 2.3.1: Model and experimental results

The lower curve in Figure 2.3.1b represents the lower boundary, while the upper curve represents the upper boundary. After the experiment is conducted on the setup, these results are visualized in the same figure by the blue data points. These follow the same procedure regarding lower and upper boundary. As can be seen, for the shortest pendulum lengths there is no upper boundary present. The reason for this is that the upper frequency corresponding to these lengths is above the maximum frequency reachable with the setup.

Discussion

The expected and the observed results seen in Figure 2.3.1b generally behave similar for different pendulum lengths. However, for essentially all cases the observed instability domain is narrower than the expected instability domain. This difference can have several causes.

First of all a simplification has been made in the stability analysis model. As explained in section 1.3, pivot acceleration has been reduced to a piecewise constant function. In practice, however, this is not the case; the acceleration is defined by an approximate sinusoidal function.
Next to that, the pendulum is modelled to have a constant length. However, for this setup the rope functions both as mass oscillator and as part of the pendulum. This means the difference between minimum and maximum pendulum length is equal to the diameter of the driving wheel, which is 0.10 m. This difference can play a significant role in the analysis.

Besides that has the pendulum been modelled as completely rigid. This means all motion from the driving wheel is assumed to be perfectly transferred to the mass. In practice, however, the rope is not fully rigid, meaning the modelled ideal situation cannot be achieved.
Also, the length change of the rope as a result of the angle it makes with the line of actuation is being disregarded in the theoretical analysis, while in practice it does occur. As a result, the applied oscillation in the experiment is not a perfect sinusoidal function with amplitude 0.05 m. This may also stimulate a difference between the modelled and observed results.
Lastly, there is possible inconsistency in the human interpretation which can negatively influence experimental results. Because this setup does not include high-end equipment to measure instability or regulate frequency, this is done by simple visualization. It may be the case that the pendulum became unstable slightly earlier or later than was observed. Or, that the supplied voltage to the driving wheel was a tenth lower or higher; this value fluctuates slightly in time.

The above imperfections presumably act together to ultimately create a difference between expected and observed results in Figure 2.3.1b. Only one of them, however, is related to the model developed in the stability analysis. The others are all related to either the simple experimental setup or human interference. Also, the difference is relatively small; in general the expected and observed results display a similar behaviour. It can therefore be concluded that by using this simplified experiment the stability analysis model has been verified and can be used for future actions.

3 Pendulum simulation

Besides a stability analysis based on linear system stability conditions, one can also simulate the behaviour of an inverted pendulum. This can for example be done using an Ordinary Differential Equation (ODE) solver in Matlab to solve the differential equations representing the state space model. A possible advantage of this approach compared to the previously used method is that it does not necessarily require simplifications such as a piecewise constant acceleration. Instead, a pure sinusoidal input can be used if desired. Also, by later generating a basin of attraction, one can estimate the probability that a theoretically stable inverted pendulum actually stabilizes in practice.

3.1 Deriving the state space model

In order to simulate the pendulum behaviour in Matlab, its state space model is required. In order to derive this model, as starting point Equation 1.9 is taken. Then, variables x_1 and x_2 and their time derivatives are defined as

$$x_1 = \varphi \quad \text{and} \quad x_2 = \dot{\varphi} \tag{3.1}$$

$$\dot{x}_1 = \dot{\varphi} \quad \text{and} \quad \dot{x}_2 = \ddot{\varphi} \tag{3.2}$$

Now, by combining these definitions of x_1 and x_2 with Equation 1.9, one can obtain the following expressions for $\dot{x}_1$ and $\dot{x}_2$:

$$\dot{x}_1 = x_2 \tag{3.3}$$

$$\dot{x}_2 = \frac{1}{L}(g + \ddot{s})\sin(x_1) - \lambda x_2 \tag{3.4}$$

where $\ddot{s}(t) = -A\omega^2 sin(\omega t)$. The differential equations presented in Equation 3.3 and Equation 3.4 form the state space model, which in the next section are going to be solved using an ODE solver in Matlab.

3.2 Solving ordinary differential equations using Matlab

In Matlab, the ode45 solver is being used to solve the differential equations forming the state space model. The full code used for this can be observed in section C.2. Besides a function in which the state space model is defined, the ODE solver also requires a time range and initial conditions as simulation input. The time duration is chosen to be 50 seconds, which is found to be more than enough for all kinds of simulations with varying parameters. Step size is chosen to be 0.01 second, which allows for sufficient detail in the simulation. The required initial conditions relate to x_1 and x_2, or in other words initial amplitude and angular velocity are defined. For an arbitrarily chosen set of parameters $A = 0.04$ m, $L = 0.10$ m and $\omega = 30$ rad/s and 50 rad/s with initial conditions $[x_1 \quad x_2]^T = [0.1 \quad 0]^T$, the pendulum behaviour has been simulated. This can be observed in Figure 3.2.1. In Figure 3.2.1a, an angular frequency ω of 30 rad/s has been applied. The amplitude clearly keeps decreasing in time, implying an unstable behaviour. The amplitude in Figure 3.2.1b, on the other hand, converges to zero in time. This means the pendulum is stable for this parameter combination. Here, an angular frequency ω of 50 rad/s has been applied. It can be concluded that 30 rad/s is below the stable threshold frequency and 50 rad/s is above the stable threshold frequency for this specific chosen set of parameters and initial conditions.

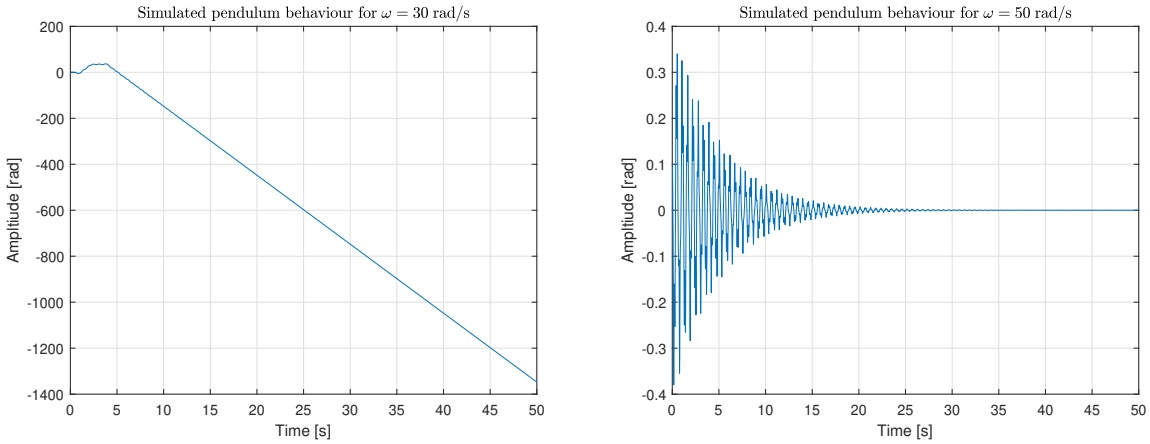

(a) Unstable simulation

(b) Stable simulation

Figure 3.2.1: Pendulum simulations for A = 0.04 m, L = 0.10 m and varying ω

3.3 Comparison to stability analysis model

In order to execute a simple model verification, the results of the pendulum simulation can be compared to the results of the previously built stability analysis model. This can be done by comparing the stability threshold frequencies from the two models to each other. However, to compare these to each other, first two minor modifications should be made. The stability analysis model is based on a piecewise constant acceleration, so this should also be incorporated in the state space model. This happens in lines 29 to 41 in the Matlab script displayed in section C.2. Besides that should the stability analysis model, which was focusing on instability earlier, be adapted to determine stability instead. This is done by repeating the steps from section 1.2 and section 1.3 to obtain the correct matrix $B(t)$ for stability in the top position. Continuing with the previously chosen parameters, a new stability analysis is then performed. Its resulting visualization can be seen in Figure 3.3.1.

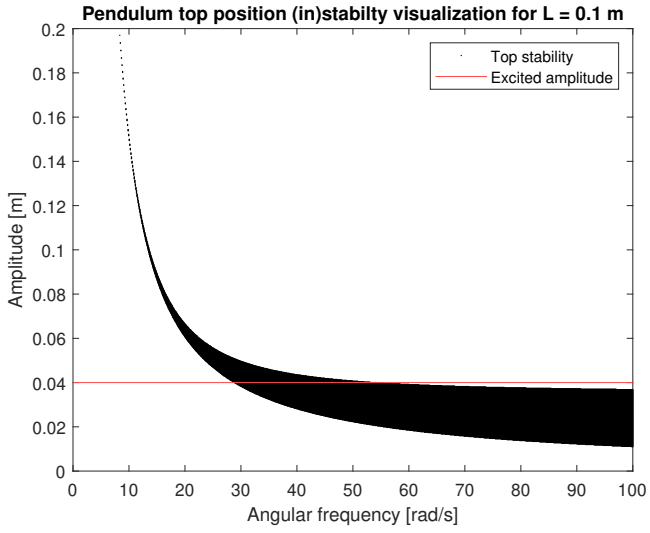

Figure 3.3.1: Pendulum top position (in)stability for varying oscillation amplitude and frequency

For this comparison, only the in red highlighted amplitude of 0.04 m is taken into account. As can be seen, there is a turnover frequency where the pendulum changes from unstable (white) to stable (black). This frequency is at 28.9 rad/s for this specific situation. Now, with the same parameters

the pendulum is simulated using the ODE solver in Matlab. This method should result in a turnover frequency which is somewhat related to already obtained turnover frequency. The pendulum is given a small initial amplitude of 0.01 radians. The resulting response slightly below and slightly above the turnover frequency can be observed in Figure 3.3.2.

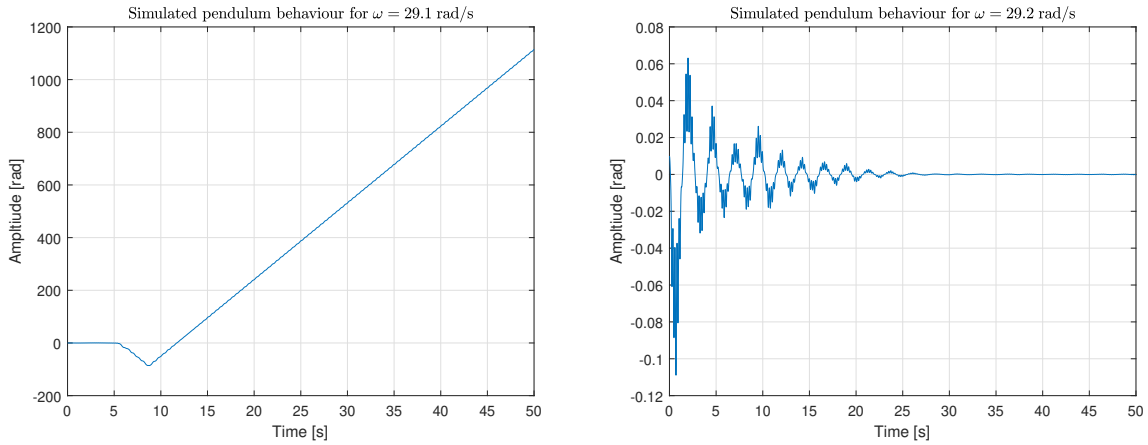

(a) Unstable simulation ($\omega = 29.1$ rad/s)

(b) Stable simulation ($\omega = 29.2$ rad/s)

Figure 3.3.2: Pendulum simulations below and above the stability threshold frequency

As can be seen, by using this method the turnover frequency is somewhere between 29.1 rad/s and 29.2 rad/s. This is close to the previously obtained frequency of 28.9 rad/s. From Figure 3.3.1 it can also be concluded that there is a maximum frequency threshold at which the inverted pendulum becomes unstable again. This value is being compared in a similar manner as for the minimum frequency threshold. The stability analysis model generates an angular frequency of 54.2 rad/s, while simulation of the pendulum leads to a frequency in between 49.8 rad/s and 49.9 rad/s. The difference between the two methods here is slightly larger than for the minimum threshold frequency. However, as can be seen in Figure 3.3.1, the maximum threshold frequency position is also more vulnerable to small differences than the minimum position. At the maximum threshold frequency, and amplitude marked in red, the slope of the top side of the black stability area is low. This means a slight difference between the models can cause big changes in the intersection frequency of the red line and the top side of the black area. The minimum threshold frequency location is less vulnerable to differences because it has a steeper slope, and so small differences do not have major effects.

From these comparison results it can be concluded that the pendulum simulation using an ODE forms a valid approximation of the real situation, since it coincides with the previously validated model. The method is now, together with the stability analysis model, going to be used to design an experimental setup. To strive for results which are as close as possible to reality, the pivot acceleration behaviour is changed back to purely sinusoidal instead of a piecewise constant function. The full process is described in the next section.

4 Inverted pendulum stabilization experimental setup

In the previous chapters, a model and a simulation have been developed which describe the theoretical stability of an inverted pendulum. In this chapter, this knowledge is going to be used to design and build an experimental setup driving an inverted pendulum. Then, the theoretical expectations from the model and simulation are being compared to the stability results obtained in practice by means of an experiment.

4.1 Investigate practical setup parameters

The first step in the design process of an inverted pendulum setup is to determine appropriate setup parameters. These parameters should be chosen in such a way that the stabilization phenomenon can be visualized with a low-budget setup. This is done using the previously developed models and simulation.

In this phase, the aim is to obtain practical values for pendulum length and oscillation amplitude. To maintain the dimensions within a practical range, a constraint is made up for the pendulum length; it can be 0.10 m at minimum and 0.30 m at maximum. In the setup, the pendulum will not be a point mass. Instead, it is going to be a rigid bar with an equal mass distribution along its length. This means its center of mass will be equal to the geometric center of the pendulum, which is halfway its length. Therefore, a pendulum of e.g. 0.30 m will be modelled as a point mass of 0.15 m.

For the range of lengths available, Figure 4.1.1 can be used to make a rough estimate of which oscillation amplitudes could result in stability. The figure follows from the stability analysis model which has been developed as first. As can be seen, in the figure amplitudes 0.02 m and 0.04 m have been highlighted in red. According to Figure 4.1.1a, a pendulum with minimum length (0.10 m) can become stable when oscillating the pivot sufficiently fast at amplitude 0.02 m. Figure 4.1.1b implies that also a pendulum with maximum length (0.30 m) can become stable when oscillating its pivot sufficiently fast at amplitude 0.04 m. It is therefore expected that when the setup allows for these two amplitudes, all pendulum lengths between 0.10 m and 0.30 m can be stabilized in inverted position. This expectation goes with the assumption that the setup can create sufficient angular velocity to reach the stability region. For this first and rough simulation, the damping coefficient has been estimated to a value $\lambda = 0.5$. Once the setup has been realized, the coefficient will be determined more accurately. According to the theoretical models, an inverted pendulum of length 0.10 m, oscillated with amplitude 0.02 m should become stable somewhere in a range from 40.8 rad/s (first model, piecewise acceleration) to 51.3 rad/s (simulation, sinusoidal acceleration). At first glance, these values seem achievable in practice. It is therefore decided to continue with the discussed dimensions to design an experimental setup.

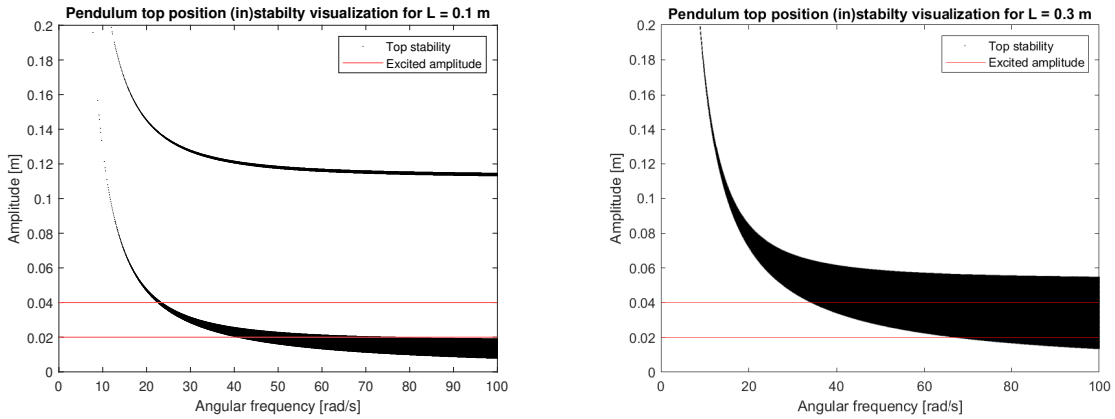

(a) 0.1 m (in)stability

(b) 0.3 m (in)stability

Figure 4.1.1: Pendulum (in)stability for minimum and maximum pendulum length

4.2 Design, manufacture and assemble the setup

After the most important design parameters are known, the experimental setup can be designed in detail. The final assembly CAD drawing can be observed in Figure 4.2.2 and the realized assembly can be seen in Figure B.0.2. The process towards this assembly will be explained part by part in this section.

Power unit and angular velocity

An important condition provided in section 4.1 is that the setup should be able to generate sufficient angular velocity to achieve stability. Therefore, the first design step is to look at the power units available for the low-budget setup. A 24V DC motor [5] is available at no cost, together with a power supply which can provide up to 20V. At no load, if this maximum voltage is supplied to the motor it spins at approximately 27 rad/s. As explained in section 4.1, it may be the case that a frequency of at least 51.3 rad/s is required for the smallest pendulum size to stabilize. Because the motor will be loaded due of inertia and friction, it is decided to implement a safety margin in the maximum achievable frequency. Therefore, a transmission ratio of 1:3 is implemented, which theoretically means the pivot can be oscillated with an angular frequency of 81 rad/s. This will likely not be achievable in practice. For practical reasons, the transmission ratio is going to be implemented by using two gears with gear ratio 1:3. More specific, the two gears will have 75 and 25 teeth, respectively, with modulus 1.25 mm. The gears will be actuated by a D-shaped shaft.

Driving mechanism

In order to transfer rotational movement of the motor into translational movement of the pendulum, a crank mechanism is going to be used. However, an ordinary crank mechanism does not have a pure sinusoidal amplitude because of rod angularity. The connecting rod makes an angle with the line of actuation and, as a result, it is slightly shorter when it is at an angle than when it is perfectly aligned with the line of actuation. One possible way of compensating this effect is by making the connecting rod extremely long, which decreases the angle significantly. However, for this setup the available space is limited, so this option is disregarded.

Instead, the crank wheel is being separated into two wheels; one purely for rotation and one for defining the amplitude. In this way, the crank wheel can have a variable radius, and so a variable amplitude, depending on the angular position of the wheel. This allows to compensate for length change of the connecting rod, which ensures a pure sinusoidal amplitude. This outer wheel is fixed to the outside world and contains two different slots, which correspond to an amplitude of 0.02 m (inner slot) and 0.04 m (outer slot). One can switch between the two amplitudes by changing the slot to which the connecting rod is attached. The inner wheel is rotating at the desired angular velocity and contains one straight slot to push the connecting rod around. Similar to the gears, it is actuated using a D-shaft. Both wheels can be observed in Figure 4.2.1.

(a) Outer wheel, defining radius

(b) Inner wheel attached, providing rotation

Figure 4.2.1: Two separate wheels, together forming a variable radius crank wheel

Guiding mechanism and supporting construction

The pendulum's pivot requires a linear guiding mechanism. This can be provided in several ways. For this setup, it is decided to use flexures to fulfill this task. Similar to the gears and the double crank wheel, they are easily 3D-printable. This significantly reduces production costs. Besides, flexures lack the presence of friction or play. This can be advantageous for the experimental setup because it can bring the practical situation closer to the theoretical modelled and simulated situation.

Lastly, to connect all designed parts a main frame is designed. This main frame is screwed to a wooden base plate, which together with the main frame forms the supporting construction. The wooden base plate is fixed to the outside world via two F-clamps. All parts, except for the wooden base plate and DC motor, are being 3D printed from PLA material. The pendulum itself is being produced in five different sizes: 0.10 m, 0.15 m, 0.20 m, 0.25 m and 0.30 m. The design has been made symmetric, so the parts are not subjected to bending or torsional forces. This can be seen more clearly in the front view shown in Figure 4.2.2b.

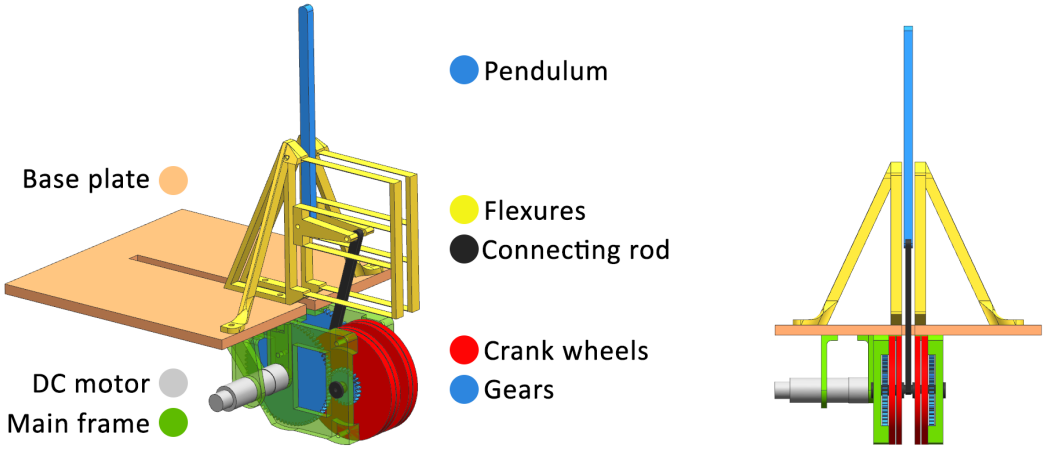

(a) All parts labeled with colours

(b) Front view

Figure 4.2.2: Final assembly CAD drawing

4.3 Experimental results and discussion

Once the experimental setup has been fully built, it can be verified to what extend the setup behaves as expected. In order to do so, first a similar preparation as for the earlier conducted experiment is necessary. The damping coefficient of each pendulum size is required, which will be obtained in a similar manner as explained in section 2.2. The setup shown in Figure 4.2.2 is turned upside down to create a free path for the pendulum, which is then given an initial amplitude, after which it is released and monitored until it stabilizes at its bottom position. The obtained data is analyzed and compared with an analytical solution resulting from a chosen damping coefficient. This results in similar graphs as visualized in Figure 2.2.1b. The resulting damping coefficients have, together with the approximate swing durations, been put in Table A.1.

Experimental results

The damping coefficients obtained earlier can now be implemented in the previously created model and simulation. In that way, a theoretical stabilization frequency can be obtained for several inverted pendulums with different lengths. An experiment is then conducted in which the supplied voltage to the motor is increased until the inverted pendulum in the setup stabilizes. This action is performed separately

for every different pendulum length. Length 0.10 m has been stabilized using an amplitude of 0.02 m, length 0.15 m once using amplitude 0.02 m and once using amplitude 0.04 m and lengths 0.20 m, 0.25 m and 0.30 have been stabilized using an amplitude of 0.04 m. The resulting stabilization frequency can, together with the theoretically expected values, be observed in Figure 4.3.1. As explained, length 0.15 m contains two different sets of frequencies since this length was stabilized using two different amplitudes.

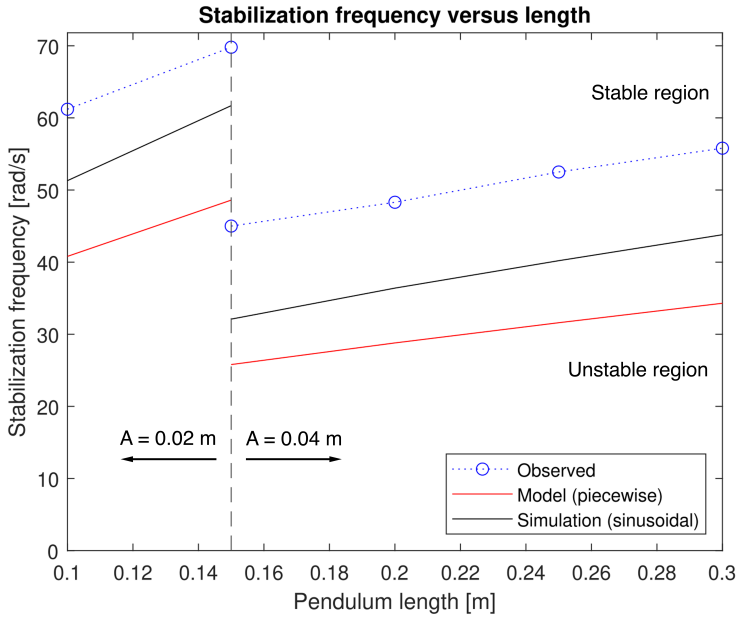

Figure 4.3.1: Experimental results

Discussion

Based on Figure 4.3.1, various conclusions can be drawn. First of all, it may be concluded that both the model and the simulation proved to be an adequate tool to design an inverted pendulum setup. The parameters which resulted from both theoretical results led to an experimental setup which was able to visualize inverted pendulum stability. Secondly, it may be concluded that both the model and the simulation react approximately similar to pendulum length and oscillation amplitude changes as happens in reality. With increasing length, the required frequency for inverted pendulum stability gradually increases if the amplitude remains equal. When the amplitude increases (0.02 m to 0.04 m at length 0.15 m), the desired frequency for stabilization significantly drops.

Besides, it may be concluded that the simulation provides a better representation of reality than the model. A possible reason for this is that the model uses a piecewise constant function for pivot acceleration, while the simulation uses a pure sinusoidal function. The latter forms a closer representation to what happens in practice. Despite a close theoretical correlation between model and reality, the simulation and the observed results still show a relatively large deviation. A reason for this can be all kinds of disturbances which play a role in reality, but are not incorporated in the ideal simulation.

The sensitivity to these disturbances can be explained using a basin of attraction. In such a visualization, (in)stability is graphed as a function of the initial conditions. On the x-axis, an array of possible initial conditions x_o is given and on the y-axis an array of conditions $\dot{x}_0$ is given. These combinations of initial conditions are then provided to the ODE solver in the simulation. If the provided initial conditions lead to a theoretically stable inverted pendulum, the combination is marked with a black dot in the graph. This means if the black, stable area is small the pendulum is sensitive to disturbances; the chance that it will be stable in practice is limited. When the black area is relatively large, this means the pendulum is more likely to be stable in practice.

For pendulum length 0.30 m, three approximations to basins of attraction have been made. In reality, all stable black points should connect to each other, since isolated stable 'islands' are not possible. However, these ideal basins of attraction require large computational power, which to such extend is not available for this project. Therefore, only approximations of a basin of attraction have been created, in which isolated stable points are visible. For this specific pendulum length, the simulation predicts the stabilization frequency to be $\omega = 43.8$ rad/s. In the experiment, the frequency was observed to be $\omega = 55.8$ rad/s. An approximation of a basin of attraction is made for these two frequencies, together with frequency $\omega = 49.8$ rad/s, which is exactly in the middle. The graphs can be observed in Figure 4.3.2.

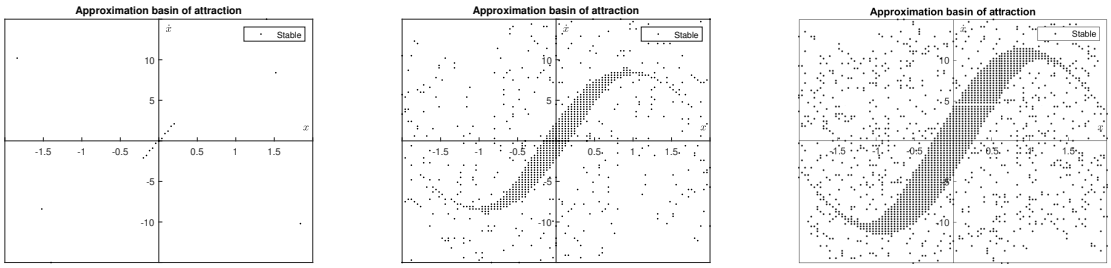

(a) $\omega = 43.8$ rad/s (b) $\omega = 49.8$ rad/s (c) $\omega = 55.8$ rad/s

Figure 4.3.2: Approximation of a basin of attraction for different oscillation frequencies

The general trend which can be observed from the basin of attraction approximations is that the stable area increases with increasing frequency within this frequency range. When looking at Figure 4.3.2a, it can be concluded that this frequency is mainly stable in an ideal situation, as the black area is only limited. This means the configuration is sensitive to disturbances, which supports the instability in practice. This is in contrast with the practically stable frequency, of which the basin of attraction approximation is shown in Figure 4.3.2c. The dark area is relatively large, which means the configuration is less sensitive to disturbances and the chance of practical stability is high. Figure 4.3.2b, which is based on the frequency half-way between theoretically and practically stable, also shows a relatively large stability area. However, the experiment turned out that this area does not suffice to overcome the disturbances present in practice.

With this known, a last comment can be made on Figure 4.3.1. If the initial conditions of the simulation were chosen such that they match a stable point in Figure 4.3.2c but not in Figure 4.3.2a and Figure 4.3.2b, the data point would have been substantially closer to the observed point as it is right now. Since these exact initial conditions, together with the disturbances, are unknown, the absolute difference between modelled, simulated and observed results in Figure 4.3.1 should be interpreted with caution.

Conclusion

This project set out three main objectives: to create and validate a model that captures the inverted pendulum stability phenomenon, to develop a simulation that mimics an inverted pendulum and to design and realize a working experimental setup based on the theoretical results.

The results documented in chapter 1 and chapter 2 have shown that the first objective has been accomplished. Although the created model uses a simplification in the form of a piecewise constant acceleration, the validation experiment, based on instability of a pendulum in bottom position, showed that the model approximates reality reasonably well. It could therefore be used to first validate the simulation results and later develop the experimental setup.

Besides the created model, also the computer simulation developed in chapter 3 has proven to be reasonably accurate. To validate the simulation model, first a piecewise constant acceleration was applied and resulting stabilization frequencies were compared to those of the earlier verified model. After it became clear that the simulation provided similar results as the model, the second objective had also been achieved. Then, time dependent acceleration in the simulation was changed for sinusoidal acceleration because the intended experimental setup also used sinusoidal acceleration.

In order to accomplish the project's third objective, appropriate experimental setup parameters were determined within the imposed size constraints using the results from the stability analysis model and simulation. These parameters formed the starting point to create a full CAD design of the experimental setup, after which it was mostly 3D printed and assembled. It turned out that the various pendulum sizes could, just as predicted, all be stabilized using the two chosen amplitudes of 0.02 m and 0.04 m and the chosen transmission ratio for angular velocity. This completes the project's third objective, but although modelled, simulated and experimental results showed the same behaviour, there was a significant difference between. Unknown disturbances and exact initial conditions were given as main reason for this observation.

All in all, it may be concluded that all three objectives set for this project are met and that the stability phenomenon of an inverted pendulum has been investigated, described and demonstrated successfully. For a future project, a possible next step is to improve the experimental setup so the amount of disturbances is reduced. In this way, model, simulation and experiments should not only show similar behaviour, but also closely show similar results.

Bibliography

[1] Andrew Stephenson. XX. On induced stability. *The London, Edinburgh, and Dublin Philosophical Magazine and Journal of Science*, 15(86):233–236, 1908.

[2] P L Kapitza. Dynamic stability of the pendulum with vibrating suspension point. *Soviet Physics–JETP*, 21(5):588–597, 1951.

[3] Eugene I. Butikov. Analytical expressions for stability regions in the Ince–Strutt diagram of Mathieu equation. *American Journal of Physics*, 86(4):259–261, 4 2018.

[4] VEGAS Pro 16, 2018.

[5] Escap HD11 216 E 204 5 - 24V DC Motor.

A Main text elaboration

A.1 Equation of motion full derivation

The starting point for this derivation of the pendulum's equation of motion is Equation 1.8. In this situation, the only relevant generalized coordinate is φ. Also, the non conservative force factor F_{nc} can be reduced to only a damping factor d, which is linearly dependent on and works in opposite direction of angular velocity $\dot{\varphi}$. This means Equation 1.8 can be rewritten to:

$$\frac{d}{dt}\left(\frac{\partial \mathcal{L}}{\partial \dot{\varphi}}\right) - \frac{\partial \mathcal{L}}{\partial \varphi} = -d\dot{\varphi} \tag{A.1}$$

All parts in this equation will now be treated separately in order to derive the equation of motion in a structured manner. For clarification purposes, the Lagrangian given in Equation 1.7 is repeated here once again. So:

$$\mathcal{L} = \frac{1}{2}M(\dot{\varphi}^2 L^2 - 2\dot{\varphi}\sin(\varphi)L\dot{s} + \dot{s}^2) - Mg(\cos(\varphi)L + s) \tag{A.2}$$

First, the Lagrangian is differentiated with respect to $\dot{\varphi}$:

$$\frac{\partial \mathcal{L}}{\partial \dot{\varphi}} = M(L^2\dot{\varphi} - \sin(\varphi)L\dot{s}) \tag{A.3}$$

Subsequent, to obtain the first term of Equation A.1, this derivative is differentiated with respect to time:

$$\frac{d}{dt}\left(\frac{\partial \mathcal{L}}{\partial \dot{\varphi}}\right) = M(L^2\ddot{\varphi} - \sin(\varphi)L\ddot{s} - \dot{\varphi}\cos(\varphi)L\dot{s}) \tag{A.4}$$

In order to get the second term of Equation A.1, the Lagrangian shown in Equation A.2 is differentiated with respect to φ:

$$\frac{\partial \mathcal{L}}{\partial \varphi} = M(-\dot{\varphi}\cos(\varphi)L\dot{s}) - Mg(-\sin(\varphi)L) = M(-\dot{\varphi}\cos(\varphi)L\dot{s} + g\sin(\varphi)L) \tag{A.5}$$

Now, Equation A.4 and Equation A.5 can be substituted in Equation A.1 to get:

$$M(L^2\ddot{\varphi} - \sin(\varphi)L\ddot{s} - \dot{\varphi}\cos(\varphi)L\dot{s}) - M(-\dot{\varphi}\cos(\varphi)L\dot{s} + g\sin(\varphi)L) = -d\dot{\varphi}$$

which can be rewritten to the final equation of motion:

$$\ddot{\varphi} + \lambda\dot{\varphi} - \frac{1}{L}(g + \ddot{s})\sin(\varphi) = 0 \tag{A.6}$$

where the new damping factor λ is defined as:

$$\lambda = \frac{d}{ML^2} \tag{A.7}$$

A.2 Equilibrium positions derivation

To find the pendulum's equilibrium positions, Equation 1.10 is being used.

$$\frac{dE_p}{d\varphi} = -Mg\sin(\varphi) = 0 \tag{A.8}$$

Solving this equation leads to equilibrium positions $\varphi = 0 + k \cdot 2\pi$ and $\varphi = \pi + k \cdot 2\pi$

A.3 Linearization around bottom position

As a starting point for the linearization process, the equation of motion presented in Equation A.6 is taken. Now, to linearize this equation, the angle the pendulum makes is regarded as a constant angle plus a small time dependent perturbation. This implies $\varphi = \theta_0 + \theta_1(t)$, where in this case $\theta_0 = \pi$ because the equation is linearized around the bottom equilibrium position. This definition of φ can now be substituted into Equation A.6 to get:

$$\ddot{\theta}_1 + \lambda\dot{\theta}_1 - \frac{1}{L}(g + \ddot{s})\sin(\pi + \theta_1) = 0$$

By applying the sum formula for a sine, this can be rewritten to:

$$\ddot{\theta}_1 + \lambda\dot{\theta}_1 - \frac{1}{L}(g + \ddot{s})(\sin(\pi)\cos(\theta_1) + \cos(\pi)\sin(\theta_1)) = 0$$

Since the perturbation $\theta_1(t)$ is very small, $\sin(\theta_1) \approx \theta_1$. This means the final linearized equation of motion is equal to:

$$\ddot{\theta}_1 + \lambda\dot{\theta}_1 + \frac{1}{L}(g + \ddot{s})\theta_1 = 0 \tag{A.9}$$

A.4 Damping coefficient per pendulum length

Table A.1: Swing duration and resulting damping coefficient per pendulum length

Pendulum length [m]	Swing duration [s]	Damping coefficient
0.10	4.0	2.20
0.15	5.5	1.70
0.20	21.0	0.38
0.25	19.0	0.45
0.30	18.5	0.50

B Supporting pictures

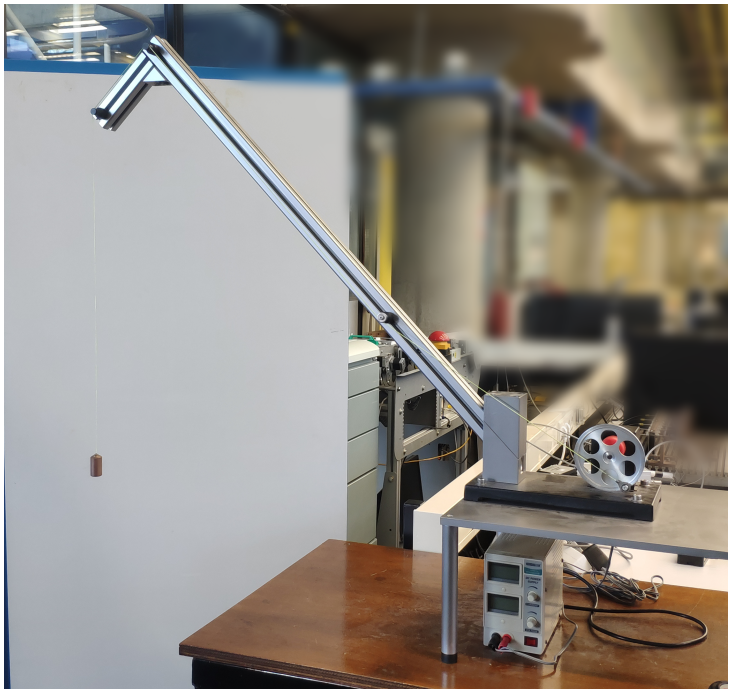

Figure B.0.1: Experimental setup Motion laboratory

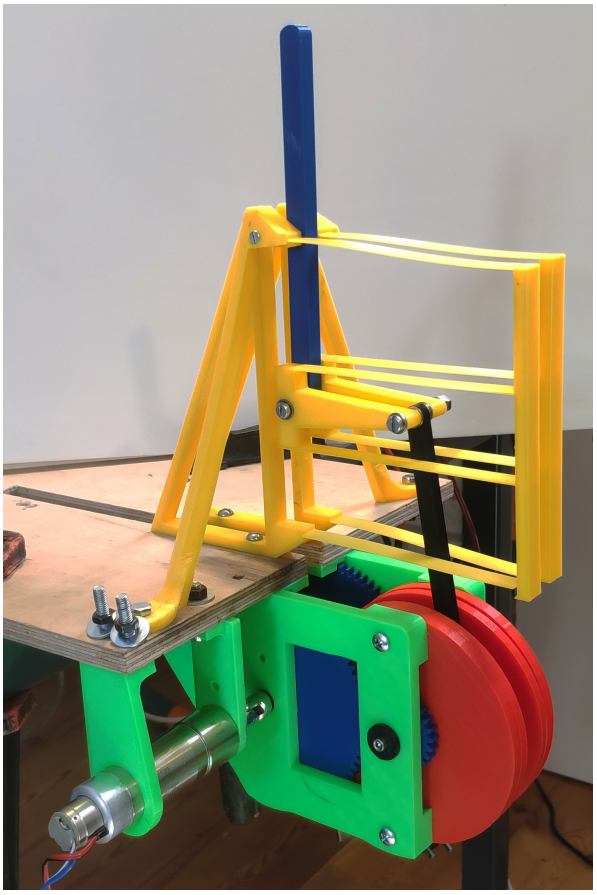

Figure B.0.2: Realized experimental setup

C Matlab

C.1 Stability analysis script

```
clear all; close all; clc;
%% Constants
n = 1000;                                           % calculation step size, [-]
m = 1;                                              % to create array later, [-]
g = 9.81;                                           % grav acceleration, [m/s^2]
d = 0.1;                                            % damping coefficient [-]

%% Variables oscillation
w_min = 0.01;                                       % minimum w, [rad/s]
w_max = 50;                                         % maximum w, [rad/s]

a_min = 0;                                          % minimum a, [m]
a_max = 0.3;                                        % maximum a, [m]

%% Variables pendulum
L = 0.5;                                            % length, [m]

%% Resulting variables
w = w_min:(w_max-w_min)/n:w_max;                    % array of w
a = a_min:(a_max-a_min)/n:a_max;                    % array of a
w_n = w/(sqrt(g/L));                                % normalized w
T = (2*pi)./w;                                      % period, [s]

%% Calculations
for i = 1:n+1
    for j = 1:n+1
        B1 = [0 1; -(1/L)*(g-w(j)^2*a(i)) -d];      % matrix B1
        B2 = [0 1; -(1/L)*(g+w(j)^2*a(i)) -d];      % matrix B2

        if max(abs(eig(expm(B2*T(j)/2)*expm(B1*T(j)/2)))) > 1       % instable
            data(1,m) = w_n(j);                     % fraction of eigenfrequency
            data(2,m) = a(i);                       % amplitude
            m=m+1;
        end
    end
end

figure(1)
plot(data(1,:),data(2,:),'.k','MarkerSize',1)
xlabel('$\omega/\omega_0 \;\textrm{[-]}$','interpreter','latex')
ylabel('$A \;\textrm{[m]}$','interpreter','latex')
title('Pendulum (in)stabilty visualization for L = 0.5 m')
legend('Instability')
```

C.2 Pendulum simulation script

```
clear all; close all; clc;

opts = odeset('MaxStep',1e-2);
%% Constants
t = [0:0.01:500];   % time vector
x0 = [0.1;0];       % initial conditions

%% Solve using ode
[t2, sol_45] = ode45(@pendulum_dyn,t,x0,opts);

%% Graph
figure(1)
plot(t2,sol_45(:,1))
grid
xlabel('Time [s]')
ylabel('Ampltiude [rad]')
title('Simulated pendulum behaviour')

%% Define function for pendulum dynamics
function dx = pendulum_dyn(t,x)

%% Constants
l = 0.1;            % length pivot to pendulum center of mass
A = 0.04;           % exitation amplitude
w = 50;             % exitation angular frequency
d = 0.4;            % damping coefficient
g = 9.81;           % gravitational constant

T = 2*pi/w;         % period of the oscillation
t_n = t/T;          % normalized time by dividing by T
t_int = floor(t_n); % floor the normalized time
t_n2 = t_n-t_int;   % subtract integer to get a value <1

%% Define oscillation behaviour
s = A*sin(w*t);     % s function, not used in function

if t_n2 < 0.5       % if piecewise approximation
    sin_approx = 1; % is used, this happens here.
else                % 0<=t_n2<0.5 means 0<=t<T/2
    sin_approx = -1;% 0.5<=t_n2<1 means T/2<=t<T
end

s_doubledot = -A*w^2*sin(w*t); % apply for sinusoidal input
% s_doubledot = -A*w^2*sin_approx; % apply for piecewise input

%% Pendulum behaviour
dx = [x(2,1); (sin(x(1,1))/l)*(g+s_doubledot)-d*x(2,1)];

end
```